

Determination of the strong coupling constant from the inclusive jet cross section in $p\bar{p}$ collisions at $\sqrt{s} = 1.96$ TeV

V.M. Abazov³⁷, B. Abbott⁷⁵, M. Abolins⁶⁵, B.S. Acharya³⁰, M. Adams⁵¹, T. Adams⁴⁹, E. Aguilo⁶, M. Ahsan⁵⁹, G.D. Alexeev³⁷, G. Alkhalaf⁴¹, A. Alton^{64,a}, G. Alverson⁶³, G.A. Alves², L.S. Ancu³⁶, M. Aoki⁵⁰, Y. Arnaud¹⁴, M. Arov⁶⁰, A. Askew⁴⁹, B. Åsman⁴², O. Atramentov^{49,b}, C. Avila⁸, J. BackusMayes⁸², F. Badaud¹³, L. Bagby⁵⁰, B. Baldin⁵⁰, D.V. Bandurin⁵⁹, S. Banerjee³⁰, E. Barberis⁶³, A.-F. Barfuss¹⁵, P. Baringer⁵⁸, J. Barreto², J.F. Bartlett⁵⁰, U. Bassler¹⁸, D. Bauer⁴⁴, S. Beale⁶, A. Bean⁵⁸, M. Begalli³, M. Begel⁷³, C. Belanger-Champagne⁴², L. Bellantoni⁵⁰, J.A. Benitez⁶⁵, S.B. Beri²⁸, G. Bernardi¹⁷, R. Bernhard²³, I. Bertram⁴³, M. Besançon¹⁸, R. Beuselinck⁴⁴, V.A. Bezzubov⁴⁰, P.C. Bhat⁵⁰, V. Bhatnagar²⁸, G. Blazey⁵², S. Blessing⁴⁹, K. Bloom⁶⁷, A. Boehnlein⁵⁰, D. Boline⁶², T.A. Bolton⁵⁹, E.E. Boos³⁹, G. Borissov⁴³, T. Bose⁶², A. Brandt⁷⁸, R. Brock⁶⁵, G. Brooijmans⁷⁰, A. Bross⁵⁰, D. Brown¹⁹, X.B. Bu⁷, D. Buchholz⁵³, M. Buehler⁸¹, V. Buescher²⁵, V. Bunichev³⁹, S. Burdin^{43,c}, T.H. Burnett⁸², C.P. Buszello⁴⁴, P. Calfayan²⁶, B. Calpas¹⁵, S. Calvet¹⁶, E. Camacho-Pérez³⁴, J. Cammin⁷¹, M.A. Carrasco-Lizarraga³⁴, E. Carrera⁴⁹, W. Carvalho³, B.C.K. Casey⁵⁰, H. Castilla-Valdez³⁴, S. Chakrabarti⁷², D. Chakraborty⁵², K.M. Chan⁵⁵, A. Chandra⁵⁴, E. Cheu⁴⁶, S. Chevalier-Théry¹⁸, D.K. Cho⁶², S.W. Cho³², S. Choi³³, B. Choudhary²⁹, T. Christoudias⁴⁴, S. Cihangir⁵⁰, D. Claes⁶⁷, J. Clutter⁵⁸, M. Cooke⁵⁰, W.E. Cooper⁵⁰, M. Corcoran⁸⁰, F. Couderc¹⁸, M.-C. Cousinou¹⁵, D. Cutts⁷⁷, M. Cwiok³¹, A. Das⁴⁶, G. Davies⁴⁴, K. De⁷⁸, S.J. de Jong³⁶, E. De La Cruz-Burelo³⁴, K. DeVaughan⁶⁷, F. Déliot¹⁸, M. Demarteau⁵⁰, R. Demina⁷¹, D. Denisov⁵⁰, S.P. Denisov⁴⁰, S. Desai⁵⁰, H.T. Diehl⁵⁰, M. Diesburg⁵⁰, A. Dominguez⁶⁷, T. Dorland⁸², A. Dubey²⁹, L.V. Dudko³⁹, L. Dufflot¹⁶, D. Duggan⁴⁹, A. Duperrin¹⁵, S. Dutt²⁸, A. Dyshkant⁵², M. Eads⁶⁷, D. Edmunds⁶⁵, J. Ellison⁴⁸, V.D. Elvira⁵⁰, Y. Enari¹⁷, S. Eno⁶¹, H. Evans⁵⁴, A. Evdokimov⁷³, V.N. Evdokimov⁴⁰, G. Facini⁶³, A.V. Ferapontov⁷⁷, T. Ferbel^{61,71}, F. Fiedler²⁵, F. Filthaut³⁶, W. Fisher⁵⁰, H.E. Fisk⁵⁰, M. Fortner⁵², H. Fox⁴³, S. Fuess⁵⁰, T. Gadfort⁷⁰, C.F. Galea³⁶, A. Garcia-Bellido⁷¹, V. Gavrilov³⁸, P. Gay¹³, W. Geist¹⁹, W. Geng^{15,65}, D. Gerbaudo⁶⁸, C.E. Gerber⁵¹, Y. Gershtein^{49,b}, D. Gillberg⁶, G. Ginther^{50,71}, G. Golovanov³⁷, B. Gómez⁸, A. Goussiou⁸², P.D. Grannis⁷², S. Greder¹⁹, H. Greenlee⁵⁰, Z.D. Greenwood⁶⁰, E.M. Gregores⁴, G. Grenier²⁰, Ph. Gris¹³, J.-F. Grivaz¹⁶, A. Grohsjean¹⁸, S. Grünendahl⁵⁰, M.W. Grünewald³¹, F. Guo⁷², J. Guo⁷², G. Gutierrez⁵⁰, P. Gutierrez⁷⁵, A. Haas^{70,d}, P. Haefner²⁶, S. Hagopian⁴⁹, J. Haley⁶³, I. Hall⁶⁵, R.E. Hall⁴⁷, L. Han⁷, K. Harder⁴⁵, A. Harel⁷¹, J.M. Hauptman⁵⁷, J. Hays⁴⁴, T. Hebbeker²¹, D. Hedin⁵², J.G. Hegeman³⁵, A.P. Heinson⁴⁸, U. Heintz⁶², C. Hensel²⁴, I. Heredia-De La Cruz³⁴, K. Herner⁶⁴, G. Hesketh⁶³, M.D. Hildreth⁵⁵, R. Hirosky⁸¹, T. Hoang⁴⁹, J.D. Hobbs⁷², B. Hoeneisen¹², M. Hohlfield²⁵, S. Hossain⁷⁵, P. Houben³⁵, Y. Hu⁷², Z. Hubacek¹⁰, N. Huske¹⁷, V. Hynek¹⁰, I. Iashvili⁶⁹, R. Illingworth⁵⁰, A.S. Ito⁵⁰, S. Jabeen⁶², M. Jaffré¹⁶, S. Jain⁷⁵, K. Jakobs²³, D. Jamin¹⁵, R. Jesik⁴⁴, K. Johns⁴⁶, C. Johnson⁷⁰, M. Johnson⁵⁰, D. Johnston⁶⁷, A. Jonckheere⁵⁰, P. Jonsson⁴⁴, A. Juste⁵⁰, E. Kajfasz¹⁵, D. Karmanov³⁹, P.A. Kasper⁵⁰, I. Katsanos⁶⁷, V. Kaushik⁷⁸, R. Kehoe⁷⁹, S. Kermiche¹⁵, N. Khalatyan⁵⁰, A. Khanov⁷⁶, A. Kharchilava⁶⁹, Y.N. Kharzheev³⁷, D. Khatidze⁷⁷, M.H. Kirby⁵³, M. Kirsch²¹, J.M. Kohli²⁸, A.V. Kozelov⁴⁰, J. Kraus⁶⁵, A. Kumar⁶⁹, A. Kupco¹¹, T. Kurča²⁰, V.A. Kuzmin³⁹, J. Kvita⁹, F. Lacroix¹³, D. Lam⁵⁵, S. Lammers⁵⁴, G. Landsberg⁷⁷, P. Lebrun²⁰, H.S. Lee³², W.M. Lee⁵⁰, A. Leflat³⁹, J. Lellouch¹⁷, L. Li⁴⁸, Q.Z. Li⁵⁰, S.M. Lietti⁵, J.K. Lim³², D. Lincoln⁵⁰, J. Linnemann⁶⁵, V.V. Lipaev⁴⁰, R. Lipton⁵⁰, Y. Liu⁷, Z. Liu⁶, A. Lobodenko⁴¹, M. Lokajicek¹¹, P. Love⁴³, H.J. Lubatti⁸², R. Luna-Garcia^{34,e}, A.L. Lyon⁵⁰, A.K.A. Maciel², D. Mackin⁸⁰, P. Mättig²⁷, R. Magaña-Villalba³⁴, P.K. Mal⁴⁶, S. Malik⁶⁷, V.L. Malyshev³⁷, Y. Maravin⁵⁹, B. Martin¹⁴, J. Martínez-Ortega³⁴, R. McCarthy⁷², C.L. McGivern⁵⁸, M.M. Meijer³⁶, A. Melnitchouk⁶⁶, L. Mendoza⁸, D. Menezes⁵², P.G. Mercadante⁴, M. Merkin³⁹, A. Meyer²¹, J. Meyer²⁴, N.K. Mondal³⁰, R.W. Moore⁶, T. Moulik⁵⁸, G.S. Muanza¹⁵, M. Mulhearn⁸¹, O. Mundal²², L. Mundim³, E. Nagy¹⁵, M. Naimuddin²⁹, M. Narain⁷⁷, R. Nayyar²⁹, H.A. Neal⁶⁴, J.P. Negret⁸, P. Neustroev⁴¹, H. Nilsen²³, H. Nogima³, S.F. Novaes⁵, T. Nunnemann²⁶, G. Obrant⁴¹, D. Onoprienko⁵⁹, J. Orduna³⁴, N. Osman⁴⁴, J. Osta⁵⁵, R. Otec¹⁰, G.J. Otero y Garzón¹, M. Owen⁴⁵, M. Padilla⁴⁸, P. Padley⁸⁰, M. Pangilinan⁷⁷, N. Parashar⁵⁶, V. Parihar⁶², S.-J. Park²⁴, S.K. Park³², J. Parsons⁷⁰, R. Partridge⁷⁷, N. Parua⁵⁴, A. Patwa⁷³, B. Penning⁵⁰, M. Perfilov³⁹, K. Peters⁴⁵, Y. Peters⁴⁵, P. Pétroff¹⁶, R. Piegai¹, J. Piper⁶⁵, M.-A. Pleier⁷³, P.L.M. Podesta-Lerma^{34,f}, V.M. Podstavkov⁵⁰, Y. Pogorelov⁵⁵, M.-E. Pol², P. Polozov³⁸, A.V. Popov⁴⁰, M. Prewitt⁸⁰, S. Protopopescu⁷³, J. Qian⁶⁴, A. Quadt²⁴, B. Quinn⁶⁶, M.S. Rangel¹⁶, K. Ranjan²⁹, P.N. Ratoff⁴³, I. Razumov⁴⁰, P. Renkel⁷⁹, P. Rich⁴⁵, M. Rijssenbeek⁷², I. Ripp-Baudot¹⁹, F. Rizatdinova⁷⁶, S. Robinson⁴⁴, M. Rominsky⁷⁵, C. Royon¹⁸, P. Rubinov⁵⁰, R. Ruchti⁵⁵, G. Safronov³⁸, G. Sajot¹⁴, A. Sánchez-Hernández³⁴, M.P. Sanders²⁶, B. Sanghi⁵⁰, G. Savage⁵⁰, L. Sawyer⁶⁰, T. Scanlon⁴⁴, D. Schaile²⁶, R.D. Schamberger⁷², Y. Scheglov⁴¹, H. Schellman⁵³, T. Schliephake²⁷,

S. Schlobohm⁸², C. Schwanenberger⁴⁵, R. Schwienhorst⁶⁵, J. Sekaric⁵⁸, H. Severini⁷⁵, E. Shabalina²⁴, M. Shamim⁵⁹, V. Shary¹⁸, A.A. Shchukin⁴⁰, R.K. Shivpuri²⁹, V. Simak¹⁰, V. Sirotenko⁵⁰, P. Skubic⁷⁵, P. Slattery⁷¹, D. Smirnov⁵⁵, G.R. Snow⁶⁷, J. Snow⁷⁴, S. Snyder⁷³, S. Söldner-Rembold⁴⁵, L. Sonnenschein²¹, A. Sopczak⁴³, M. Sosebee⁷⁸, K. Soustruznik⁹, B. Spurlock⁷⁸, J. Stark¹⁴, V. Stolin³⁸, D.A. Stoyanova⁴⁰, J. Strandberg⁶⁴, M.A. Strang⁶⁹, E. Strauss⁷², M. Strauss⁷⁵, R. Ströhmer²⁶, D. Strom⁵¹, L. Stutte⁵⁰, S. Sumowidagdo⁴⁹, P. Svoisky³⁶, M. Takahashi⁴⁵, A. Tanasijczuk¹, W. Taylor⁶, B. Tiller²⁶, M. Titov¹⁸, V.V. Tokmenin³⁷, I. Torchiani²³, D. Tsybychev⁷², B. Tuchming¹⁸, C. Tully⁶⁸, P.M. Tuts⁷⁰, R. Unalan⁶⁵, L. Uvarov⁴¹, S. Uvarov⁴¹, S. Uzunyan⁵², P.J. van den Berg³⁵, R. Van Kooten⁵⁴, W.M. van Leeuwen³⁵, N. Varelas⁵¹, E.W. Varnes⁴⁶, I.A. Vasilyev⁴⁰, P. Verdier²⁰, L.S. Vertogradov³⁷, M. Verzocchi⁵⁰, M. Vesterinen⁴⁵, D. Vilanova¹⁸, P. Vint⁴⁴, P. Vokac¹⁰, R. Wagner⁶⁸, H.D. Wahl⁴⁹, M.H.L.S. Wang⁷¹, J. Warchol⁵⁵, G. Watts⁸², M. Wayne⁵⁵, G. Weber²⁵, M. Weber^{50,g}, A. Wenger^{23,h}, M. Wetstein⁶¹, A. White⁷⁸, D. Wicke²⁵, M.R.J. Williams⁴³, G.W. Wilson⁵⁸, S.J. Wimpenny⁴⁸, M. Wobisch⁶⁰, D.R. Wood⁶³, T.R. Wyatt⁴⁵, Y. Xie⁷⁷, C. Xu⁶⁴, S. Yacoub⁵³, R. Yamada⁵⁰, W.-C. Yang⁴⁵, T. Yasuda⁵⁰, Y.A. Yatsunenko³⁷, Z. Ye⁵⁰, H. Yin⁷, K. Yip⁷³, H.D. Yoo⁷⁷, S.W. Youn⁵⁰, J. Yu⁷⁸, C. Zeitnitz²⁷, S. Zelitch⁸¹, T. Zhao⁸², B. Zhou⁶⁴, J. Zhu⁷², M. Zielinski⁷¹, D. Zieminska⁵⁴, L. Zivkovic⁷⁰, V. Zutshi⁵², and E.G. Zverev³⁹

(The DØ Collaboration)

- ¹Universidad de Buenos Aires, Buenos Aires, Argentina
²LAFEX, Centro Brasileiro de Pesquisas Físicas, Rio de Janeiro, Brazil
³Universidade do Estado do Rio de Janeiro, Rio de Janeiro, Brazil
⁴Universidade Federal do ABC, Santo André, Brazil
⁵Instituto de Física Teórica, Universidade Estadual Paulista, São Paulo, Brazil
⁶University of Alberta, Edmonton, Alberta, Canada; Simon Fraser University, Burnaby, British Columbia, Canada; York University, Toronto, Ontario, Canada and McGill University, Montreal, Quebec, Canada
⁷University of Science and Technology of China, Hefei, People's Republic of China
⁸Universidad de los Andes, Bogotá, Colombia
⁹Center for Particle Physics, Charles University, Faculty of Mathematics and Physics, Prague, Czech Republic
¹⁰Czech Technical University in Prague, Prague, Czech Republic
¹¹Center for Particle Physics, Institute of Physics, Academy of Sciences of the Czech Republic, Prague, Czech Republic
¹²Universidad San Francisco de Quito, Quito, Ecuador
¹³LPC, Université Blaise Pascal, CNRS/IN2P3, Clermont, France
¹⁴LPSC, Université Joseph Fourier Grenoble 1, CNRS/IN2P3, Institut National Polytechnique de Grenoble, Grenoble, France
¹⁵CPPM, Aix-Marseille Université, CNRS/IN2P3, Marseille, France
¹⁶LAL, Université Paris-Sud, IN2P3/CNRS, Orsay, France
¹⁷LPNHE, IN2P3/CNRS, Universités Paris VI and VII, Paris, France
¹⁸CEA, Irfu, SPP, Saclay, France
¹⁹IPHC, Université de Strasbourg, CNRS/IN2P3, Strasbourg, France
²⁰IPNL, Université Lyon 1, CNRS/IN2P3, Villeurbanne, France and Université de Lyon, Lyon, France
²¹III. Physikalisches Institut A, RWTH Aachen University, Aachen, Germany
²²Physikalisches Institut, Universität Bonn, Bonn, Germany
²³Physikalisches Institut, Universität Freiburg, Freiburg, Germany
²⁴II. Physikalisches Institut, Georg-August-Universität Göttingen, Göttingen, Germany
²⁵Institut für Physik, Universität Mainz, Mainz, Germany
²⁶Ludwig-Maximilians-Universität München, München, Germany
²⁷Fachbereich Physik, University of Wuppertal, Wuppertal, Germany
²⁸Panjab University, Chandigarh, India
²⁹Delhi University, Delhi, India
³⁰Tata Institute of Fundamental Research, Mumbai, India
³¹University College Dublin, Dublin, Ireland
³²Korea Detector Laboratory, Korea University, Seoul, Korea
³³SungKyunKwan University, Suwon, Korea
³⁴CINVESTAV, Mexico City, Mexico
³⁵FOM-Institute NIKHEF and University of Amsterdam/NIKHEF, Amsterdam, The Netherlands
³⁶Radboud University Nijmegen/NIKHEF, Nijmegen, The Netherlands
³⁷Joint Institute for Nuclear Research, Dubna, Russia
³⁸Institute for Theoretical and Experimental Physics, Moscow, Russia
³⁹Moscow State University, Moscow, Russia
⁴⁰Institute for High Energy Physics, Protvino, Russia

- ⁴¹*Petersburg Nuclear Physics Institute, St. Petersburg, Russia*
⁴²*Stockholm University, Stockholm, Sweden, and Uppsala University, Uppsala, Sweden*
⁴³*Lancaster University, Lancaster, United Kingdom*
⁴⁴*Imperial College London, London SW7 2AZ, United Kingdom*
⁴⁵*The University of Manchester, Manchester M13 9PL, United Kingdom*
⁴⁶*University of Arizona, Tucson, Arizona 85721, USA*
⁴⁷*California State University, Fresno, California 93740, USA*
⁴⁸*University of California, Riverside, California 92521, USA*
⁴⁹*Florida State University, Tallahassee, Florida 32306, USA*
⁵⁰*Fermi National Accelerator Laboratory, Batavia, Illinois 60510, USA*
⁵¹*University of Illinois at Chicago, Chicago, Illinois 60607, USA*
⁵²*Northern Illinois University, DeKalb, Illinois 60115, USA*
⁵³*Northwestern University, Evanston, Illinois 60208, USA*
⁵⁴*Indiana University, Bloomington, Indiana 47405, USA*
⁵⁵*University of Notre Dame, Notre Dame, Indiana 46556, USA*
⁵⁶*Purdue University Calumet, Hammond, Indiana 46323, USA*
⁵⁷*Iowa State University, Ames, Iowa 50011, USA*
⁵⁸*University of Kansas, Lawrence, Kansas 66045, USA*
⁵⁹*Kansas State University, Manhattan, Kansas 66506, USA*
⁶⁰*Louisiana Tech University, Ruston, Louisiana 71272, USA*
⁶¹*University of Maryland, College Park, Maryland 20742, USA*
⁶²*Boston University, Boston, Massachusetts 02215, USA*
⁶³*Northeastern University, Boston, Massachusetts 02115, USA*
⁶⁴*University of Michigan, Ann Arbor, Michigan 48109, USA*
⁶⁵*Michigan State University, East Lansing, Michigan 48824, USA*
⁶⁶*University of Mississippi, University, Mississippi 38677, USA*
⁶⁷*University of Nebraska, Lincoln, Nebraska 68588, USA*
⁶⁸*Princeton University, Princeton, New Jersey 08544, USA*
⁶⁹*State University of New York, Buffalo, New York 14260, USA*
⁷⁰*Columbia University, New York, New York 10027, USA*
⁷¹*University of Rochester, Rochester, New York 14627, USA*
⁷²*State University of New York, Stony Brook, New York 11794, USA*
⁷³*Brookhaven National Laboratory, Upton, New York 11973, USA*
⁷⁴*Langston University, Langston, Oklahoma 73050, USA*
⁷⁵*University of Oklahoma, Norman, Oklahoma 73019, USA*
⁷⁶*Oklahoma State University, Stillwater, Oklahoma 74078, USA*
⁷⁷*Brown University, Providence, Rhode Island 02912, USA*
⁷⁸*University of Texas, Arlington, Texas 76019, USA*
⁷⁹*Southern Methodist University, Dallas, Texas 75275, USA*
⁸⁰*Rice University, Houston, Texas 77005, USA*
⁸¹*University of Virginia, Charlottesville, Virginia 22901, USA and*
⁸²*University of Washington, Seattle, Washington 98195, USA*
(Dated: Received 13 November 2009; published 29 December, 2009)

We determine the strong coupling constant α_s and its energy dependence from the p_T dependence of the inclusive jet cross section in $p\bar{p}$ collisions at $\sqrt{s} = 1.96$ TeV. The strong coupling constant is determined over the transverse momentum range $50 < p_T < 145$ GeV. Using perturbative QCD calculations to order $\mathcal{O}(\alpha_s^3)$ combined with $\mathcal{O}(\alpha_s^4)$ contributions from threshold corrections, we obtain $\alpha_s(M_Z) = 0.1161^{+0.0041}_{-0.0048}$. This is the most precise result obtained at a hadron-hadron collider.

PACS numbers: 13.87.-a, 12.38.Qk, 13.87.Ce

Asymptotic freedom, the fact that the strong force between quarks and gluons keeps getting weaker when it is probed at increasingly small distances, is a remarkable property of quantum chromodynamics (QCD). This property is reflected by the renormalization group equation (RGE) prediction for the dependence of the strong coupling constant α_s on the renormalization scale μ_r and therefore on the momentum transfer. Experimental tests of asymptotic freedom require precise determinations of $\alpha_s(\mu_r)$ over a large range of momentum trans-

fer. Frequently, α_s has been determined using production rates of hadronic jets in either e^+e^- annihilation or in deep-inelastic ep scattering (DIS) [9]. So far there exists only a single α_s result from inclusive jet production in hadron-hadron collisions. The CDF Collaboration determined α_s from the inclusive jet cross section in $p\bar{p}$ collisions at $\sqrt{s} = 1.8$ TeV obtaining $\alpha_s(M_Z) = 0.1178^{+0.0081}_{-0.0095}(\text{exp.})^{+0.0071}_{-0.0047}(\text{scale}) \pm 0.0059(\text{PDF})$ [10].

In this article we determine α_s and its dependence on the momentum transfer using the published measure-

ment of the inclusive jet cross section [11, 12] with the D0 detector [13] at the Fermilab Tevatron Collider in $p\bar{p}$ collisions at $\sqrt{s} = 1.96$ TeV. The inclusive jet cross section $d^2\sigma_{\text{jet}}/dp_T d|y|$ was measured using the Run II iterative midpoint cone algorithm [14] with a cone radius of 0.7 in rapidity, y , and azimuthal angle. Rapidity is related to the polar scattering angle θ with respect to the beam axis by $y = 0.5 \ln [(1 + \beta \cos \theta)/(1 - \beta \cos \theta)]$ with $\beta = |\vec{p}|/E$. The measurement comprises 110 data points corrected to the particle level [15] and presented as a function of the momentum component transverse to the beam direction, p_T , for $p_T > 50$ GeV in six regions of $|y|$ for $0 < |y| < 2.4$.

The ingredients of perturbative QCD (pQCD) calculations in hadron collisions are α_s , the perturbative coefficients c_n (in the n -th power of α_s), and the parton distribution functions (PDFs). Conceptually, PDFs depend only on the hadron momentum fraction x carried by the parton and on the factorization scale μ_f . In practice, PDFs are determined from measurements of observables which depend on α_s . Therefore resulting PDF parametrizations depend on the assumption for α_s made in the extraction procedure. For all precise phenomenology, this implicit α_s dependence must be taken into account consistently. The pQCD prediction for the inclusive jet cross section can therefore be written as

$$\sigma_{\text{pert}}(\alpha_s) = \left(\sum_n \alpha_s^n c_n \right) \otimes f_1(\alpha_s) \otimes f_2(\alpha_s), \quad (1)$$

where the sum runs over all powers n of α_s which contribute to the calculation ($n = 2, 3, 4$ in this analysis, see below). The $f_{1,2}$ are the PDFs of the initial state hadrons and the “ \otimes ” sign denotes the convolution over the momentum fractions x_1, x_2 of the hadrons. Since the RGE uniquely relates the value of $\alpha_s(\mu_r)$ at any scale μ_r to the value of $\alpha_s(M_Z)$, all equations can be expressed in terms of $\alpha_s(M_Z)$. The total theory prediction for inclusive jet production is given by the pQCD result in (1) multiplied by a correction factor for nonperturbative effects

$$\sigma_{\text{theory}}(\alpha_s(M_Z)) = \sigma_{\text{pert}}(\alpha_s(M_Z)) \cdot c_{\text{nonpert}}. \quad (2)$$

The factor c_{nonpert} includes corrections due to hadronization and the underlying event which have been estimated in Ref. [11] using PYTHIA [16] with CTEQ6.5 PDFs [17], tune QW [18], and $\alpha_s(M_Z) = 0.118$. The hadronization (underlying event) corrections vary between -15% (+30%) to -3% (+6%), for $p_T = 50$ to 600 GeV [12].

The perturbative results are the sum of a full calculation to $\mathcal{O}(\alpha_s^3)$ [next-to-leading order (NLO)], combined with the $\mathcal{O}(\alpha_s^4)$ (2-loop) terms from threshold corrections [19]. Adding the 2-loop threshold corrections leads to a significant reduction in the μ_r and μ_f dependence of the calculation. The theory calculations are performed in the $\overline{\text{MS}}$ scheme [20] for five active quark flavors using the next-to-next-to-leading logarithmic (3-loop) approximation of the RGE [21, 22]. The PDFs are taken from the MSTW2008 next-to-next-to-leading order (NNLO) parametrizations [23, 24] and μ_r and μ_f are both chosen

equal to the jet p_T . The calculations use FASTNLO [25] based on NLOJET++ [26, 27] and on code from the authors of Ref. [19].

In this analysis, the value of α_s is determined from sets of inclusive jet cross section data points by minimizing the χ^2 function between data and the theory result (2) using MINUIT [28]. Where appropriate, the $\alpha_s(M_Z)$ result will be evolved to the scale p_T using the 3-loop solution of the RGE, providing a result for $\alpha_s(p_T)$. All correlated experimental and theoretical uncertainties are treated in the Hessian approach [29], except for the $\mu_{r,f}$ dependence (see below). The central $\alpha_s(M_Z)$ result is obtained by minimizing χ^2 with respect to $\alpha_s(M_Z)$ and the nuisance parameters for the correlated uncertainties. By scanning χ^2 as a function of $\alpha_s(M_Z)$, the uncertainties are obtained from the $\alpha_s(M_Z)$ values for which χ^2 is increased by 1 with respect to the minimum value.

To determine α_s according to this procedure, knowledge of $\sigma_{\text{pert}}(\alpha_s(M_Z))$ is required as a continuous function of $\alpha_s(M_Z)$, over a $\alpha_s(M_Z)$ range which covers the possible fit results and their uncertainties. This can be achieved based on a series of PDFs obtained under the same conditions but for different values of $\alpha_s(M_Z)$ using interpolation in $\alpha_s(M_Z)$. Some recent PDF analyses have applied this strategy and their results are documented for different values of $\alpha_s(M_Z)$. The MSTW2008 NNLO (NLO) PDF parametrizations [23, 24] are presented for 21 $\alpha_s(M_Z)$ values in the range 0.107 – 0.127 (0.110 – 0.130) in steps of 0.001 and the CTEQ6.6 results [30] are available for five values of $\alpha_s(M_Z) = 0.112, 0.114, 0.118, 0.122, 0.125$. Because of the wide range in $\alpha_s(M_Z)$ covered by the MSTW2008 PDFs and the fine and equidistant spacing in $\alpha_s(M_Z)$, we use cubic spline interpolation to obtain a smooth parametrization for the $\alpha_s(M_Z)$ dependence of the cross section for $0.108 \leq \alpha_s(M_Z) \leq 0.126$ ($0.111 \leq \alpha_s(M_Z) \leq 0.129$) for the NNLO (NLO) PDFs. This range is sufficient to cover our central values and the uncertainties. The MSTW2008 analysis includes data sets that have not yet been included in other global PDF analyses (DIS jet data from HERA and recent CCFR/NuTeV dimuon data); the results are available in NNLO accuracy which is adequate when including the $\mathcal{O}(\alpha_s^4)$ contributions from threshold corrections in the cross section calculation. The CTEQ6.6 PDF parametrizations are available up to NLO, for five $\alpha_s(M_Z)$ values, and for a more limited range in $\alpha_s(M_Z)$ as compared to MSTW2008. Therefore the MSTW2008 PDFs are used to obtain the main results for this analysis while the CTEQ6.6 PDFs are used for comparison.

Care must be taken in phenomenological analyses if the observable under study was already used to provide significant constraints on the PDFs as this introduces correlations of experimental and PDF uncertainties, and it may affect the sensitivity to possible new physics signals. Both aspects are relevant in this α_s determination since the D0 inclusive jet data under study is included in the MSTW2008 PDF analysis. Since the correlation of

experimental and PDF uncertainties is not documented, it can not be taken into account when using the PDFs to extract $\alpha_s(M_Z)$ from the jet data. As a consequence, we must avoid using those jet cross section data points which have provided strong PDF constraints. While the quark PDFs are constrained by precision structure function data, the only direct source of information on the high x gluon PDF comes currently from Tevatron inclusive jet data. The impact of Tevatron jet data on the gluon density is documented in Ref. [23] in Figs. 51-53. Figure 51 shows that excluding the Tevatron jet data starts to affect the gluon density at $x > 0.2 - 0.3$, while for $x \lesssim 0.25$ the difference in the gluon density with and without Tevatron jet data is less than 5%. Figure 53 shows that $x < 0.3$ is the region in which the gluon results for MSTW2008 and CTEQ6.6 are very close. We conclude that for momentum fractions $x < 0.2 - 0.3$ the Tevatron jet data do not have a significant impact on the gluon density, and therefore we can neglect correlations between PDF and experimental uncertainties for these data. Based on this constraint we select below those inclusive jet data points from which we extract α_s .

The Tevatron jet data (which access p_T above 500 GeV) are probing momentum transfers at which α_s has not yet been probed in other experiments. Therefore we can not rule out deviations in the running of α_s at large momentum due to possible new physics contributions to the RGE. Since such modifications of the RGE are not taken into account in the PDF determinations, these effects would effectively be absorbed into the PDFs. By construction, using such PDFs to extract α_s could seemingly confirm the RGE expectations, even in the presence of new physics contributions to the RGE. For a consistent α_s determination we would therefore exclude high p_T data in the region where the RGE has not yet been successfully tested which is the region of $p_T \gtrsim 200$ GeV [9]. However, those data are already removed by the restriction to $x < 0.2 - 0.3$, so no additional requirement is needed to account for this.

In $2 \rightarrow 2$ processes, given the rapidities and p_T of the two jets, one can compute the momentum fractions x_1 and x_2 carried by the initial partons. The inclusive jet cross section at given p_T and $|y|$ is, however, integrated over all additional jets in an event, so the rapidity of the other jet and therefore the full event kinematics, including x_1 and x_2 , are not known. The value of the larger momentum fraction $x_{max} = \max(x_1, x_2)$ can be computed only under an assumption for the rapidity of the unobserved jet. For each inclusive jet ($p_T, |y|$) bin we define the variable $\tilde{x} = x_T \cdot (e^{|y|} + 1)/2$ where $x_T = 2p_T/\sqrt{s}$, p_T is taken at the bin center, and $|y|$ at the lower boundary of the $|y|$ bin. This variable \tilde{x} corresponds to x_{max} for the case that the unobserved jet was produced at $y = 0$. In the pQCD calculation, for a given inclusive jet ($p_T, |y|$) bin the distribution of $x_{max} = \max(x_1, x_2)$ always has a peak plus a tail towards high x_{max} values. Although the variable \tilde{x} does not represent the peak position of the x_{max} distribution, it is correlated with

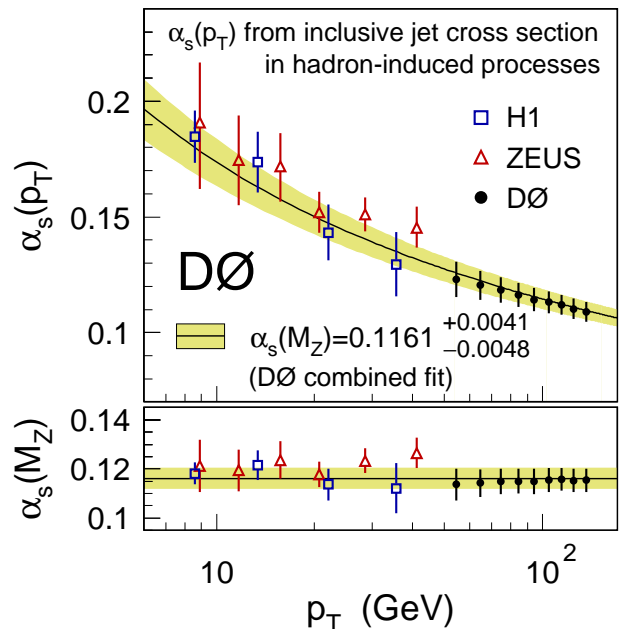


FIG. 1: The results for $\alpha_s(p_T)$ (top) and $\alpha_s(M_Z)$ (bottom). The D0 results are based on 22 selected data points which have been grouped to produce the 9 data points shown. For comparison, results from HERA DIS jet data have been included and also the RGE prediction for the combined D0 fit result and its uncertainty (line and band). All data points are shown with their total uncertainties.

that distribution. The requirement $\tilde{x} < 0.15$ removes all data points for which more than half of the cross section is produced at $x_{max} \gtrsim 0.25$. This leaves 22 (out of 110) data points for the α_s analysis with $p_T < 145$ GeV for $0 < |y| < 0.4$, $p_T < 120$ GeV for $0.4 < |y| < 0.8$, $p_T < 90$ GeV for $0.8 < |y| < 1.2$, and $p_T < 70$ GeV for $1.2 < |y| < 1.6$. Although this selection criterion is well-motivated, the specific choices of the variable \tilde{x} and the requirement $\tilde{x} < 0.15$ are somewhat arbitrary. We have therefore studied variations of the selection requirement in the range $\tilde{x} < 0.10 - 0.17$ and other choices for the definition of \tilde{x} (for example assuming that the unobserved jet has $y_2 = \pm|y|$), and, we find that the α_s results are stable within 1%. We conclude that the choice of $\tilde{x} < 0.15$ restricts the jet data to those points which receive no significant contributions from $x_{max} > 0.25$. For these data points, experimental and PDF uncertainties are treated as being uncorrelated.

In the α_s determination, we consider the uncorrelated experimental uncertainties and all 23 sources of correlated experimental uncertainties as documented in Refs. [11, 12]. The nonperturbative corrections are divided into hadronization and underlying event effects. The uncertainty for each is taken to be half the size of the corresponding effect. PDF uncertainties are computed using the 20 68% C.L. uncertainty eigenvectors as provided by MSTW2008 [23]. The uncertainties in the pQCD calculation due to uncalculated higher order

TABLE I: Central values and uncertainties due to different sources for the nine $\alpha_s(p_T)$ results and for the combined $\alpha_s(M_Z)$ result (bottom). All uncertainties are multiplied by a factor of 10^3 .

p_T range (GeV)	No. of data points	p_T (GeV)	$\alpha_s(p_T)$	Total uncertainty	Experimental uncorrelated	Experimental correlated	Nonperturb. correction	PDF uncertainty	$\mu_{r,f}$ variation
50–60	4	54.5	0.1229	+7.6 -7.7	± 0.4	+4.8 -4.9	+5.8 -5.6	+0.4 -0.6	+1.0 -1.9
60–70	4	64.5	0.1204	+6.2 -6.3	± 0.3	+4.1 -4.3	+4.5 -4.3	+0.6 -0.5	+1.3 -1.5
70–80	3	74.5	0.1184	+5.6 -5.6	± 0.3	+3.8 -3.9	+4.0 -3.9	+0.6 -0.6	+1.0 -0.9
80–90	3	84.5	0.1163	+5.1 -5.1	± 0.3	+3.6 -3.7	+3.5 -3.5	+0.7 -0.7	+0.9 -0.6
90–100	2	94.5	0.1142	+4.9 -4.9	± 0.3	+3.6 -3.6	+3.3 -3.3	+0.8 -0.8	+1.1 -0.6
100–110	2	104.5	0.1131	+4.7 -4.7	± 0.2	+3.4 -3.5	+3.1 -3.0	+0.8 -0.8	+1.1 -0.6
110–120	2	114.5	0.1121	+4.2 -4.4	± 0.2	+3.1 -3.3	+2.5 -2.7	+0.7 -0.8	+1.2 -0.7
120–130	1	124.5	0.1102	+4.4 -4.4	± 0.2	+3.2 -3.4	+2.6 -2.6	+0.9 -0.9	+1.4 -0.9
130–145	1	136.5	0.1090	+4.2 -4.3	± 0.3	+3.1 -3.4	+2.3 -2.4	+0.9 -0.9	+1.5 -0.9
50–145	22	M_Z	0.1161	+4.1 -4.8	± 0.1	+3.4 -3.3	+1.0 -1.6	+1.1 -1.2	+2.5 -2.9

contributions are estimated from the $\mu_{r,f}$ dependence of the calculations when varying the scales in the range $0.5 < \mu_{r,f}/p_T < 2$. In the kinematic region under study, variations of μ_r and μ_f have positively correlated effects on the jet cross sections. A correlated variation of both scales is therefore a conservative estimate of the corresponding uncertainty. Since the $\mu_{r,f}$ uncertainties can not be treated as Gaussian, these are not included in the Hessian χ^2 definition. Following Refs. [31, 32], the α_s fits are repeated for different choices ($\mu_{r,f} = 0.5p_T$ and $\mu_{r,f} = 2p_T$) and the differences to the central result (obtained for $\mu_{r,f} = p_T$) are taken to be the corresponding uncertainties for $\alpha_s(M_Z)$. Those are added in quadrature to the other uncertainties to obtain the total uncertainty.

Data points from different $|y|$ regions with similar p_T are grouped to determine the results for $\alpha_s(M_Z)$ and $\alpha_s(p_T)$. A combined fit to all 22 data points yields $\alpha_s(M_Z) = 0.1161^{+0.0041}_{-0.0048}$ with $\chi^2/\text{Ndf} = 17.2/21$. The results are shown in Fig. 1 as nine $\alpha_s(p_T)$ (top) and $\alpha_s(M_Z)$ values (bottom) in the range $50 < p_T < 145$ GeV with their total uncertainties which are largely correlated between the points. Also included are results at lower p_T from inclusive jet cross sections in DIS from the HERA experiments H1 [31] and ZEUS [32] and the 3-loop RGE prediction for our combined $\alpha_s(M_Z)$ result. Our $\alpha_s(p_T)$ results are consistent with the energy dependence predicted by the RGE and extend the HERA results towards higher p_T . The combined result is consistent with the result of $\alpha_s(M_Z) = 0.1189 \pm 0.0032$ from combined HERA jet data [33] and with the world average value of $\alpha_s(M_Z) = 0.1184 \pm 0.0007$ [9]. The contributions from individual uncertainty sources are listed in Table I. The largest source is the experimental correlated uncertainty for which the dominant contributions are from the jet energy calibration, the p_T resolution and the integrated luminosity.

Varying the size of the uncertainties of the nonperturbative corrections between a factor of 0.5 and 2

changes the central value by $^{+0.0003}_{-0.0010}$ and does not affect the uncertainty of the combined $\alpha_s(M_Z)$ result. Replacing the MSTW2008 NNLO PDFs by the CTEQ6.6 PDFs changes the central result by only +0.5% which is much less than the PDF uncertainty. Excluding the 2-loop contributions from threshold corrections and using pure NLO pQCD (together with MSTW2008 NLO PDFs and the 2-loop RGE) gives a result of $\alpha_s(M_Z) = 0.1202^{+0.0072}_{-0.0059}$. The small increase in the central value is a result of the missing $\mathcal{O}(\alpha_s^4)$ contributions which are compensated by a corresponding increase in α_s . The difference to the central result is well within the scale uncertainty of the NLO result. The increased uncertainty is mainly caused by the increased $\mu_{r,f}$ dependence, but also by the larger PDF uncertainty at NLO.

In summary, we have determined the strong coupling constant from the inclusive jet cross section using theory prediction in NLO plus 2-loop threshold corrections. The $\alpha_s(p_T)$ results support the energy dependence predicted by the renormalization group equation. The combined result from 22 selected data points is $\alpha_s(M_Z) = 0.1161^{+0.0041}_{-0.0048}$. This is the most precise α_s result obtained at a hadron collider.

We thank Graeme Watt for helpful discussions. We thank the staffs at Fermilab and collaborating institutions, and acknowledge support from the DOE and NSF (USA); CEA and CNRS/IN2P3 (France); FASI, Rosatom and RFBR (Russia); CNPq, FAPERJ, FAPESP and FUNDUNESP (Brazil); DAE and DST (India); Colciencias (Colombia); CONACyT (Mexico); KRF and KOSEF (Korea); CONICET and UBACyT (Argentina); FOM (The Netherlands); STFC and the Royal Society (United Kingdom); MSMT and GACR (Czech Republic); CRC Program, CFI, NSERC and WestGrid Project (Canada); BMBF and DFG (Germany); SFI (Ireland); The Swedish Research Council (Sweden); and CAS and CNSF (China).

[a] Visitor from Augustana College, Sioux Falls, SD, USA.

[b] Visitor from Rutgers University, Piscataway, NJ, USA.

- [c] Visitor from The University of Liverpool, Liverpool, UK.
- [d] Visitor from SLAC, Menlo Park, CA, USA.
- [e] Visitor from Centro de Investigacion en Computacion - IPN, Mexico City, Mexico.
- [f] Visitor from ECFM, Universidad Autonoma de Sinaloa, Culiacán, Mexico.
- [g] Visitor from Universität Bern, Bern, Switzerland.
- [h] Visitor from Universität Zürich, Zürich, Switzerland.
- [9] S. Bethke, *Eur. Phys. J. C* **64**, 689 (2009).
- [10] T. Affolder *et al.* (CDF Collaboration), *Phys. Rev. Lett.* **88**, 042001 (2002).
- [11] V. M. Abazov *et al.* (D0 Collaboration), *Phys. Rev. Lett.* **101**, 062001 (2008).
- [12] See EPAPS Document No. E-PRLTAO-101-033833 for tables of the inclusive jet cross section results and the uncertainties. For more information on EPAPS see <http://www.aip.org/pubservs/epaps.html>
- [13] V. M. Abazov *et al.* (D0 Collaboration), *Nucl. Instrum. Methods Phys. Res. A* **565**, 463 (2006).
- [14] G. C. Blazey *et al.*, in *Proceedings of the Workshop: "QCD and Weak Boson Physics in Run II"*, Batavia, Illinois, 2000, edited by U. Baur, R. K. Ellis, and D. Zepfenfeld, (FERMILAB Report No. FERMILAB-PUB-00-297), p 47, see Section 3.5.
- [15] C. Buttar *et al.*, arXiv:0803.0678, Sec. 9.
- [16] T. Sjöstrand *et al.*, *Comput. Phys. Commun.* **135**, 238 (2001).
- [17] W. K. Tung *et al.* *JHEP* **0702**, 053 (2007).
- [18] M. G. Albrow *et al.* (TeV4LHC QCD Working Group), FERMILAB Report No. FERMILAB-CONF-06-359, arXiv:hep-ph/0610012.
- [19] N. Kidonakis and J. F. Owens, *Phys. Rev. D* **63**, 054019 (2001).
- [20] W. A. Bardeen, A. J. Buras, D. W. Duke and T. Muta, *Phys. Rev. D* **18**, 3998 (1978).
- [21] O. V. Tarasov, A. A. Vladimirov and A. Y. Zharkov, *Phys. Lett. B* **93**, 429 (1980).
- [22] S. A. Larin and J. A. M. Vermaseren, *Phys. Lett. B* **303**, 334 (1993).
- [23] A. D. Martin, W. J. Stirling, R. S. Thorne and G. Watt, *Eur. Phys. J. C* **63**, 189 (2009).
- [24] A. D. Martin, W. J. Stirling, R. S. Thorne and G. Watt, *Eur. Phys. J. C* **64**, 653 (2009).
- [25] T. Kluge, K. Rabbertz and M. Wobisch, DESY Report No. DESY-06-186, FERMILAB Report No. FERMILAB-CONF-06-352-E, arXiv:hep-ph/0609285.
- [26] Z. Nagy, *Phys. Rev. D* **68**, 094002 (2003).
- [27] Z. Nagy, *Phys. Rev. Lett.* **88**, 122003 (2002).
- [28] F. James, CERN long writeup D506.
- [29] A. Cooper-Sarkar and C. Gwenlan, in *Proceedings of the Workshop: HERA and the LHC, Part A, Geneva, Switzerland, 2005*, edited by A. De Roeck and H. Jung, (CERN Report No. CERN-2005-014, DESY Report No. DESY-PROC-2005-01) see Part 2, Sec. 3.
- [30] P. M. Nadolsky *et al.*, *Phys. Rev. D* **78**, 013004 (2008).
- [31] A. Aktas *et al.* (H1 Collaboration), *Phys. Lett. B* **653**, 134 (2007).
- [32] S. Chekanov *et al.* (ZEUS Collaboration), *Phys. Lett. B* **649**, 12 (2007).
- [33] C. Glasman (H1 Collaboration and ZEUS Collaboration), *J. Phys. Conf. Ser.* **110**, 022013 (2008).